Chen, C., **Cai, W.**, **Naumov, D.**, Tu, K., Zhou, H., Zhang, Y., **Kolditz, O.**, **Shao, H.** (2021):
Numerical investigation on the capacity and efficiency of a deep enhanced U-tube borehole heat exchanger system for building heating
Renew. Energy **169** , 557 - 572

Numerical investigation on the capacity and efficiency of a deep enhanced U-tube borehole heat exchanger system for building heating

Chaofan Chen[a,b], Wanlong Cai[a,c], Dmitri Naumov[a,d], Kun Tu[e,f], Hongwei Zhou[f], Yuping Zhang[c,g], Olaf Kolditz[a,b], Haibing Shao[a,*]

[a] *Helmholtz Centre for Environmental Research-UFZ, Permoserstr. 15, Leipzig 04318, Germany*
[b] *Applied Environmental Systems Analysis, Dresden University of Technology, Dresden 01069, Germany*
[c] *School of Human Settlements and Civil engineering, Xi'an Jiaotong University, Xi'an, Shaanxi 710049 China*
[d] *Freiberg University of Mining and Technology, Freiberg 09599, Germany*
[e] *Department of Environmental Sciences, University of California, Riverside CA 92521, USA*
[f] *China University of Mining and Technology (Beijing), Beijing 100083, China*
[g] *Key Laboratory of Coal Resources Exploration and Comprehensive Utilisation, Ministry of Natural Resources, Xi'an, Shaanxi 710021, China*

Abstract

Deep geothermal energy has become widely exploited in recent years through the use of closed loop systems for building heating. Intended to meet high heating demand in densely populated neighbourhoods, an enhanced U-tube borehole heat exchanger (EUBHE) system, in which a deviated deep borehole is connected with another vertical one to form a closed loop, is introduced in this work. For capacity and efficiency analysis of applying EUBHE systems to extract deep geothermal energy, a 3D numerical model is implemented and established based on the OpenGeoSys software. Through evaluation by thermal performance tests and thermal response tests on the EUBHE system, the maximum sustainable heat extraction rate is found to be 1.2 MW in a single heating season and 1.1 MW in 10 years, which can provide heating to more than 35 000 m^2 of residential buildings located in

[*]Corresponding author

Email addresses: chaofan.chen@ufz.de (Chaofan Chen), cwl828@stu.xjtu.edu.cn (Wanlong Cai), dmitri.naumov@ufz.de (Dmitri Naumov), tukun2014@163.com (Kun Tu), zhw@cumtb.edu.cn (Hongwei Zhou), xazyp@163.com (Yuping Zhang), olaf.kolditz@ufz.de (Olaf Kolditz), haibing.shao@ufz.de (Haibing Shao)

northern China. Moreover, the 10-year system thermal performance and efficiency are evaluated when coupled with a ground source heat pump (GSHP), and compared with the two deep borehole heat exchanger (2-DBHE) array system that has the same total borehole length as the EUBHE system. Results show that GSHP-coupled EUBHE system is more efficient than the 2-DBHE array system, as it consumes 27 % less electricity.

Keywords: Geothermal energy, Building heating, Enhanced U-tube borehole heat exchanger, Long-term thermal performance, Efficiency

---

Nomenclature

Roman letters

A	pipe cross section area (m^2)
c	specific heat capacity ($\mathrm{J\,kg^{-1}\,K^{-1}}$)
d	pipe diameter (m)
D_h	hydraulic diameter of pipe (m)
f	friction factor (-)
H	heat source/sink ($\mathrm{W\,m^{-3}}$)
$\mathbf{I}$	identity matrix (-)
L	length of the borehole (m)
Nu	Nusselt number (-)
P	heat extraction rate or thermal power (W)
Pr	Prandtl number (-)
Q	flow rate ($\mathrm{m^3\,s^{-1}}$)
q_{nTs}	normal heat flux of soil/rock ($\mathrm{W\,m^{-2}}$)
r	pipe radius (m)
Re	Reynolds number (-)

T temperature (°C)

t time (s)

t_p wall thickness of pipe (m)

U overall heat transfer coefficient ($\mathrm{W\,m^{-2}\,K^{-1}}$)

v flow velocity ($\mathrm{m\,s^{-1}}$)

$\dot{W}$ electric power (W)

W electricity consumption (kWh)

z depth (m)

Greek Letters

β_L longitudinal heat dispersivity coefficient (m)

ϵ soil/rock porosity (-)

$\mathit{\Lambda}$ tensor of thermal hydrodynamic dispersion ($\mathrm{W\,m^{-1}\,K^{-1}}$)

η efficiency of circulation pump (%)

$\mathit{\Gamma}$ boundary

λ thermal conductivity ($\mathrm{W\,m^{-1}\,K^{-1}}$)

μ dynamic viscosity of circulation fluid (Pa s)

$\mathit{\Phi}$ thermal resistance ($\mathrm{W\,m^{-1}\,K^{-1}}$)

ρ density ($\mathrm{kg\,m^{-3}}$)

Operators

Δ difference operator

$\int$ integral operator

∇ nabla vector operator

Subscripts

b borehole

cp	circulation pump
f	circulation fluid
g	grout
hp	heat pump
p	pipe
s	soil/rock
w	groundwater

Abbreviations

BHE	Borehole Heat Exchanger
CSP	Coefficient of System Performance
DBHE	Deep Borehole Heat Exchanger
EUBHE	Enhanced U-tube Borehole Heat Exchanger
GSHP	Ground Source Heat Pump
TPT	Thermal Performance Test
TRT	Thermal Response Test

1. Introduction

As a renewable and clean resource, geothermal energy has been increasingly used for building heating in closed loop systems. In projects over 30 kW, ground source heat pumps (GSHP) are often coupled with a borehole heat exchanger (BHE) array to extract a large amount of heat from the shallow subsurface [1]. Recent researches have been conducted on the design optimisation [2] and long-term sustainability [3] of these shallow systems. Nevertheless, in densely populated urban areas, there is limited land available for the installation of many BHEs. In this case, deep borehole heat exchangers (DBHE) with a depth of more than 2 km can be constructed to provide heat to commercial buildings [4] and residential neighbourhoods [5]. Due to limited sustainable heat extraction rate of a single DBHE [6], it is still hard to meet heating demand for a densely populated neighbourhood, especially in northern China [7]. Therefore, engineers tend to construct multiple DBHEs that are connected by a pipe network to provide heating for newly-developed building projects [8]. However, only increasing the number of DBHEs might be not the best method to extract more deep geothermal energy for building heating because of structural limitations of DBHEs for heat exploitation [9].

Given the recent low oil prices and the resulting over-capacity in advanced drilling market at the same time, a new design for deep geothermal energy exploitation is thus proposed called an Enhanced U-tube Borehole Heat Exchange (EUBHE) system (see Fig. 1). Its design typically includes two deep boreholes to a depth of more than 2 km, with one deviated borehole connected with another vertical one at the bottom. Casing is installed in both boreholes and the entire borehole wall is cemented, forming a closed loop to extract heat from the deep subsurface.

To our knowledge, the idea of EUBHE design is not entirely new. For example, Schulz [10] has investigated the closed loop geothermal system (CLGS), which is a kind of large EUBHE system with long horizontal boreholes. Li et al. [11] established a 3D numerical model of a deep-buried pipe and studied its heat transfer, extraction, and storage capacity. Meanwhile, a similar idea has also been proposed in the geothermal industry by the company Eavor. They introduced a closed buried-pipe system (Eavor-Loop$^{\mathrm{TM}}$) that is formed by the connection of two vertical wells with many horizontal multilateral wellbores [12].

Such EUBHE systems and similar concepts do have advantages over DBHE array systems. Firstly, by connecting two deep boreholes at the bottom, the effective heat exchange area can be significantly expanded, particularly at the deep high-temperature section. Secondly, elimination of the coaxial pipe not only leads to less pressure drop of fluid circulating [13], it also increases the system thermal efficiency by removing the internal heat loss due to inner pipe [14]. However, because of increasing drilling complexity and elevated investment in constructing one EUBHE system compared with a 2-DBHE array system, several scientific and engineering questions have to be addressed before the new design can be applied in reality. For example, how much heat can be extracted via a typical EUBHE system? How does the thermal performance of a EUBHE compare with a 2-DBHE array for building heating? Will the operational cost of the EUBHE system be higher? For the building heating industry in any other potential locations, investigations on these questions are very much needed. To answer the above questions, an EUBHE model needs to be precisely established, in which the complicated borehole geometry and geothermal gradient of the

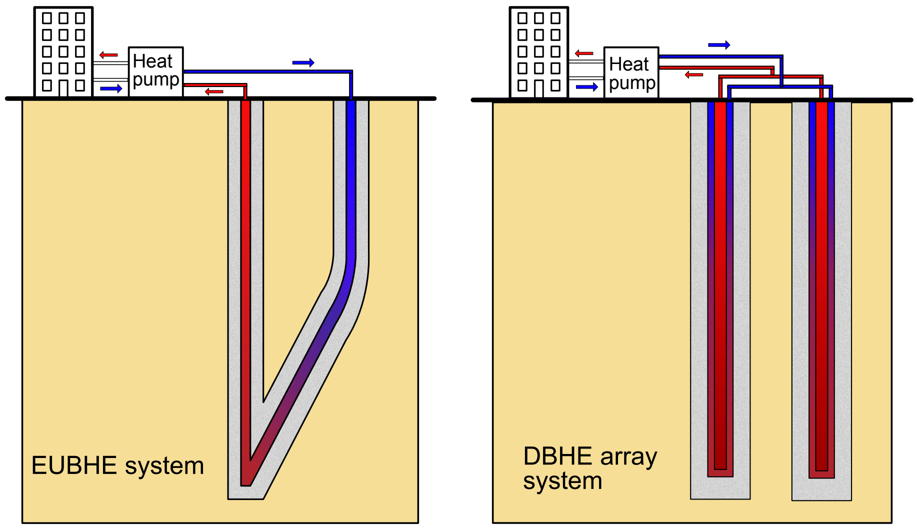

Figure 1: Structural overview of an EUBHE system and a 2-DBHE array system.

surrounding soil/rock have to be reflected.

Essentially, the thermal performance of an EUBHE system is controlled by the heat transport process between the borehole and surrounding soil/rock. Significant advances have already been achieved in the literature to analytically quantify this process. Starting from the pioneering work of Ramey Jr et al. [15], the temperature of fluid in the borehole can be calculated as a function of borehole depth and circulation time. Subsequently, Hasan et al. [16] advanced Ramey's model by considering the changing heat flux at the borehole-subsurface interface. Moreover, in order to estimate the soil/rock temperature, Eskilson [17] presented a line source model for calculating the soil temperature distribution induced by the borehole heat exchangers. Dehghan and Kukrer [18] also derived the 1D analytical expression for the specific heat transfer rate of a borehole. By coupling the heat transfer equations in the soil/rock and the borehole compartments, Beier et al. [19, 20] developed a transient model for the thermal response test on the U-tube and coaxial types of borehole heat exchangers. These analytical solutions can conveniently and efficiently calculate different types of BHEs. However, in an EUBHE system, the U-shaped borehole is surrounded by the soil/rock with non-linearly distributed temperature along the flowing direction. There is no analytical solution available to our best knowledge which is capable of predicting the transient temperature evolution caused by an EUBHE system.

Alternatively, for the large buried pipe and BHE system with distributed soil/rock temperature, many researchers investigated the system performance and efficiency by employing sophisticated numerical models. For example, Song et al. [21] numerically analysed the heat production performance of the CLGS based on the FDM model. Cui et al. [22] investigated the heat extraction rate of a horizontal well buried in hot dry rock formations and assessed its technical and economic feasibility. Li et al. [23] set up a fully discretized 3D model to study the heat transfer characteristics of the vertical deep-buried U-bend pipe. In long-term operation, Tang and Nowamooz [24] set up a 3D numerical model of the shallow BHE system and estimated its performance over five years. Larwa and Kupiec [25] studied the long-term effects of a horizontal ground heat exchanger operation. Focusing on the DBHE system, Renaud et al. [26] investigated the thermal influence and heat recovery in 30 years of production. Chen et al. [6] and Kong et al. [27] simulated the temperature evolution of inflow and outflow over the operation of 30 years by applying dual-continuum approach that was originally proposed by Al-Khoury et al. [28] and extended by Diersch et al. [29, 30].

Although both large buried pipe systems and DBHE systems can already be efficiently simulated by advanced numerical models, to the best of our knowledge, few studies evaluated the sustainable heat extraction rate of the newly proposed EUBHE system for building heating and compared the system efficiency with the DBHE array system in long-term operation for a design reference. In order to reveal the capacity and efficiency of applying EUBHE systems to extract deep geothermal energy for building heating, a 3D EUBHE numerical model was implemented based on the open-source scientific software OpenGeoSys (OGS), then verified against the analytical solution [15]. The maximum sustainable heat extraction rates of the EUBHE system in northern China in short and long terms were evaluated through conjoint analysis on Thermal Performance Test (TPT) and Thermal Response Test (TRT). Subsequently, 10-year thermal performance and system efficiency were predicted and compared with the 2-DBHE array system that has the same total borehole length as the EUBHE system. The benefits of applying the EUBHE system for building heating was also evaluated by 10-year simulations when coupled with GSHP.

2. Theoretical framework

The numerical model of the EUBHE system is constructed as shown in Fig. 2: the circulation fluid flows through the pipe, which is surrounded by

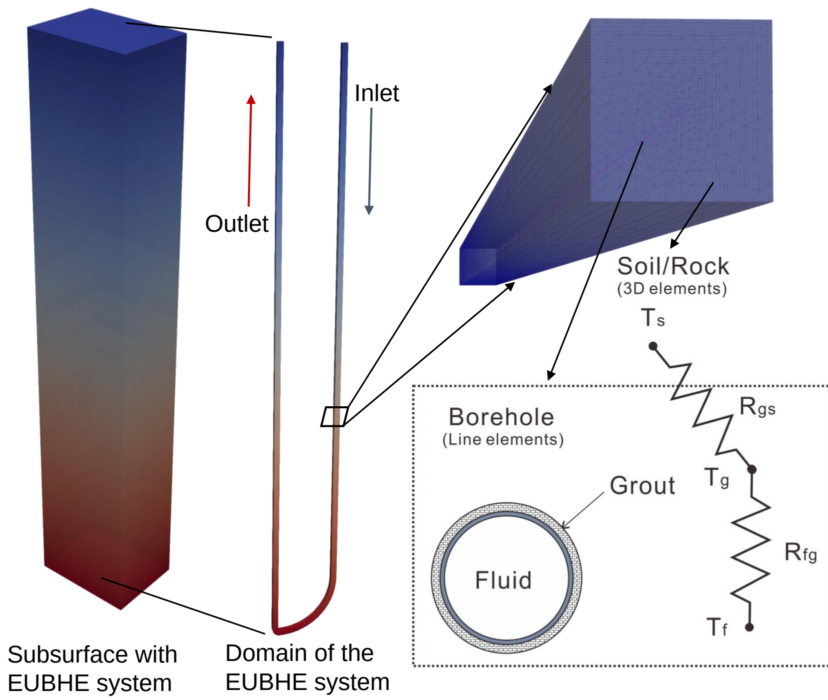

Figure 2: The numerical model of an EUBHE system in OGS.

grout and encapsulated inside the borehole. This allows fluid to exchange heat energy with the surrounding soil/rock. Following the dual-continuum approach [31], the OpenGeoSys (OGS) software [32, 33] divides the subsurface into two coupled compartments, which are the soil/rock part and the borehole part. Typically, 3D elements are used to discretize the soil/rock part, and line elements are introduced to represent the pipe and grout inside of the borehole. There are three governing equations in the borehole heat transport process, which correspond to the heat balance in each one of the compartments. With the soil/rock specific heat capacity c_s, soil/rock density ρ_s and soil/rock porosity ϵ, the soil/rock temperature evolution T_s is determined by the following governing equation considering both the heat convection and conduction,

$$[\epsilon\rho_w c_w + (1-\epsilon)\rho_s c_s]\frac{\partial T_s}{\partial t} + \nabla\cdot(\rho_w c_w \mathbf{v}_w T_s) - \nabla\cdot(\mathit{\Lambda}_s\cdot\nabla T_s) = H_s, \quad (1)$$

where c_w, ρ_w, and $\mathbf{v}_w$ refer to the specific heat capacity, density, and velocity of groundwater, respectively. $\mathit{\Lambda}_s$ denotes the tensor of thermal hydrodynamic dispersion and H_s represents the heat source and sink terms. The heat flux between soil/rock and borehole is then given by the following equation,

$$q_{nT_s} = -\Phi_{gs}\left(T_g - T_s\right) \text{ on } \Gamma_s, \tag{2}$$

where Γ_s is the boundary between soil/rock and borehole, Φ_{gs} is the thermal resistance between soil/rock part and grout component inside the borehole, and T_g is the grout temperature inside the borehole.

For the grout compartment surrounding the pipe, the heat transport process is assumed to be dominated by the heat conduction,

$$(1-\epsilon_g)\rho_g c_g \frac{\partial T_g}{\partial t} - \nabla \cdot [(1-\epsilon_g)\lambda_g \cdot \nabla T_g] = H_g \tag{3}$$

$$\text{with Robin type of BC :}$$

$$q_{nT_g} = -\Phi_{gs}\left(T_s - T_g\right) - \Phi_{fg}\left(T_f - T_g\right) \text{ on } \Gamma_g. \tag{4}$$

The heat exchange term Φ_{fg} is the thermal resistance between circulation fluid (T_f) and grout (T_g). Detailed calculation of heat exchange coefficients (Φ_{fg} and Φ_{gs}) can be found in Diersch et al. [29] and [31].

For the pipe compartment, the heat transport process is mainly dominated by the thermal convection of the circulation fluid f with a flow velocity of $\mathbf{v}_f$,

$$\rho_f c_f \frac{\partial T_f}{\partial t} + \rho_f c_f \mathbf{v}_f \cdot \nabla T_f - \nabla \cdot (\Lambda_f \cdot \nabla T_f) = H_f \tag{5}$$

$$\text{with Robin type of BC :}$$

$$q_{nT_f} = -\Phi_{fg}\left(T_g - T_f\right) \text{ on } \Gamma_f, \tag{6}$$

in which the hydrodynamic thermal dispersion tensor can be written as,

$$\Lambda_f = \left(\lambda_f + \rho_f c_f \beta_L \|\mathbf{v}_f\|\right)\mathbf{I} \tag{7}$$

where λ_f, ρ_f, c_f denote the heat conductivity, density, and specific heat capacity of the circulation fluid. In the above equation, β_L refers to the longitudinal heat dispersivity coefficient, and $\mathbf{I}$ is the identity matrix.

In the OpenGeoSys software, a dual-continuum approach has been successfully applied to solve single-U (1U), double-U (2U), and coaxial (CXA and CXC) types of BHEs (Hein et al. [34]; Chen et al. [6]; Chen et al. [35]). Also, for CXA type of the DBHE, OpenGeoSys model has been successfully validated against monitoring data (Huang et al. [36]). For the borehole heat transport process of the EUBHE design presented in this work, a new BHE type has been further implemented, in which the governing equations (1), (3), and (5) are linked together and solved in an implicit manner.

3. Numerical simulations

3.1. Model Verification

In order to verify the borehole heat transport process implemented in OpenGeoSys, a benchmark is simulated and the numerical result is compared against the analytical solution proposed by Ramey Jr et al. [15]. In this benchmark, a 30 m long pipeline (see Table 1 for its material properties) is horizontally placed in the subsurface (see Fig. 3(a)), with circulation fluid transported inside at a velocity of 0.0038 m/s. Detailed input parameters required by the benchmark are listed in Table 1. The inlet circulation fluid temperature is kept at 20 °C, and the surrounding soil/rock has an initial temperature of 55 °C. Due to the lower temperature of the injected circulation fluid, the surrounding soil/rock is gradually cooled down. Particularly, in order to illustrate in detail the impact of initial conditions in the numerical model, the initial circulation fluid and grout temperatures are set at 20 and 55 °C, respectively. The calculation of the Ramey's analytical solution for this benchmark is described in Appendix A. For detailed configuration of the numerical model for the benchmark, readers may refer to the OpenGeoSys online documentation [37].

Table 1: Detailed parameters set in the benchmark.

Parameter	Symbol	Value	Unit
Borehole diameter	d_b	0.28	m
Internal diameter of pipe	d_p	0.25826	m
Wall thickness of pipe	t_p	0.00587	m
Thermal conductivity of pipe wall	λ_p	1.3	$\mathrm{W\,m^{-1}\,K^{-1}}$
Soil/rock thermal conductivity	λ_s	2.78	$\mathrm{W\,m^{-1}\,K^{-1}}$
Heat capacity of soil/rock	$\rho_s c_s$	3.2×10^6	$\mathrm{J\,m^{-3}\,K^{-1}}$
Thermal conductivity of grout	λ_g	0.73	$\mathrm{W\,m^{-1}\,K^{-1}}$
Heat capacity of grout	$\rho_g c_g$	3.8×10^6	$\mathrm{J\,m^{-3}\,K^{-1}}$
Thermal conductivity of circulation fluid	λ_f	0.59	$\mathrm{W\,m^{-1}\,K^{-1}}$
Heat capacity of circulation fluid	$\rho_f c_f$	4.19×10^6	$\mathrm{J\,m^{-3}\,K^{-1}}$
Dynamic viscosity of circulation fluid	μ_f	1.14×10^{-3}	$\mathrm{kg\,m^{-1}\,s^{-1}}$

The simulated evolution of the outlet circulation fluid temperature over time is compared against that from the analytical solution (see Fig. 3). The main difference is concentrated at the beginning stage of the simulation, when the outlet circulation fluid temperature is affected by the initial temperature of the pipe inside the borehole and grout heat capacity in the

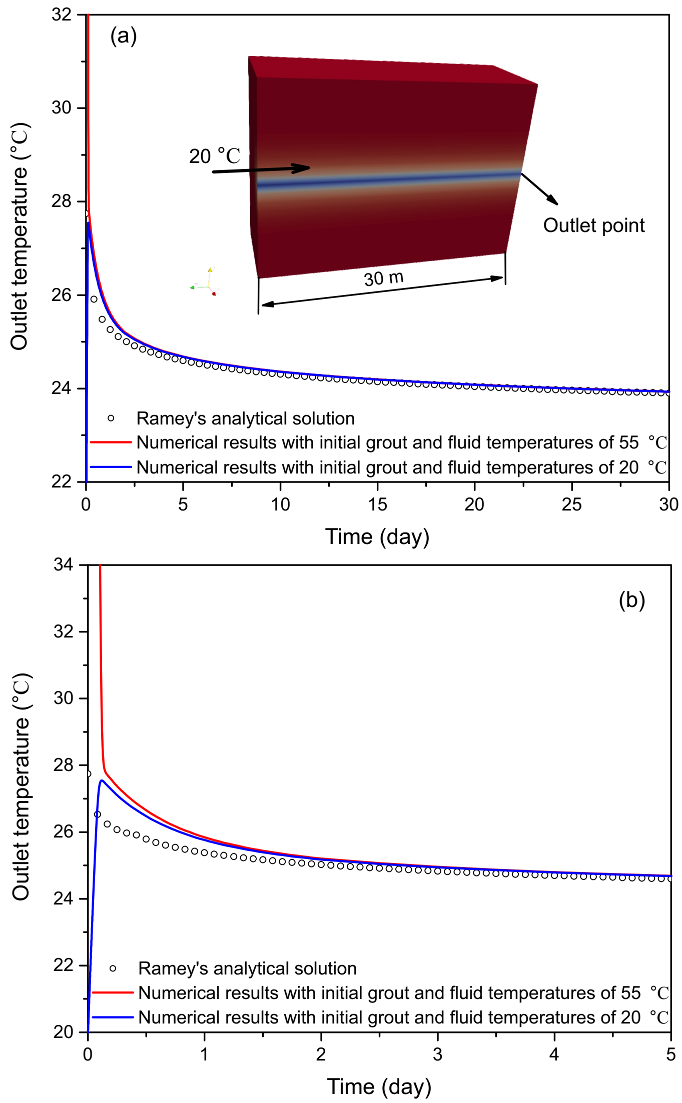

Figure 3: Change of the simulated outlet fluid temperature over (a) 30 days and (b) the first 5 days, in comparison against Ramey's analytical solution. The blue and red lines represent the numerical results with initial circulation fluid and grout temperatures of 20 °C and 55 °C, respectively. The circles are results of Ramey's analytical solution.

numerical model. Those are two differences between the numerical model and Ramey's analytical solution. Due to the initial condition of the circulation fluid and grout in the numerical model, the initial circulation fluid in the pipe takes 7894.74 seconds (a little less than 0.1 days) to be drained, while there is no such process in Ramey's analytical solution. In the analytical solution, circulation fluid temperature in the pipe is calculated to be in equilibrium with the surrounding soil/rock. It can be observed from Fig. 3(b) that due to around 0.1 days' delay in the numerical results, the numerical results are effectively shifted forward temporally (see the red line). In addition, because of consideration of the grout heat conduction in the numerical model (Eq. (3)), the circulation fluid temperature decreases more slowly than that in the analytical solution (see Appendix A). The above two differences make the numerical outlet temperatures consistently higher than those in the analytical solution in the beginning as presented in Fig. 3. However, when the simulated time is long enough, *e.g.* more than five days in Fig. 3(a), the heat transfer will be more dominated by soil/rock heat conduction and less influenced by the initial condition and grout heat capacity. Then analytical and numerical results match well as the simulated time increases.

For the circulation fluid temperature distribution along the pipe after 10 days and 30 days presented in Fig. 4, both the analytical and the numerical model predict nearly identical results. The difference in temperature is accounted to be less than 0.15 % after 30 days. With this successful verification, the borehole heat transport process of the EUBHE system can thus be predicted by the numerical model.

3.2. Model setup

3.2.1. Model domain

According to the preliminary design provided on the EUBHE system in the city of Xi'an, China [9], the horizontal distance between the two boreholes on the ground surface is 205 m and depth of the vertical borehole is 2505 m. The deviated borehole kicks off at 2355 m with an about 45-degree deviation, and is connected with the vertical borehole at the bottom. The total offset accounts for about 5200 m. In order to keep a fair comparison to the EUBHE system, a second numerical model with two 2600 m deep boreholes is constructed and connected in parallel to form an equivalent 2-DBHE array. The parameters of the EUBHE and DBHE systems are listed in Table 2. The parameter values used in our numerical model are following those reported in the experimental setup in Xi'an city [4, 9]. The subsurface

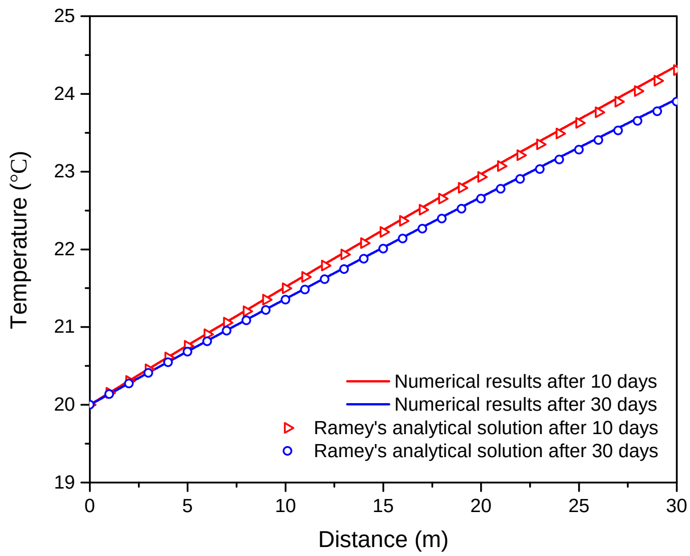

Figure 4: Comparison on the circulation fluid temperature distribution along the pipe after operation of 10 days and 30 days.

soil/rock properties are kept to be homogeneous and isotropic over the entire domain.

3.2.2. Initial and boundary conditions

For the initial and boundary conditions of the model, the ground surface temperature is set to 14.7 °C with a geothermal gradient of 0.035 °C/m according to the environmental and geological data obtained in Xi'an city [38]. The lateral boundaries are considered to be the no-heat-flux type. Three different EUBHE boundary conditions are included in simulation scenarios: constant inflow temperature, constant heat extraction rate, and constant building thermal power. The mechanisms behind the EUBHE boundary conditions are explained as follows.

- Constant inflow temperature

  With this type of boundary, the inflow temperature of EUBHE is kept constant during the whole simulation. The amount of extracted heat can be quantified dynamically by the multiplication of circulation flow rate Q_f and the temperature difference between the inflow T_i and outflow T_o (*cf.* Eq (8)). This setup is equivalent to a so-called

Table 2: Subsurface properties, EUBHE and DBHE borehole structure information, and operating parameters in numerical models.

Item	Parameter	Symbol	Value	Unit
Shared by EUBHE and DBHE	Borehole diameter	d_b	0.2159	m
	Internal diameter of pipe/outer pipe	d_p	0.178	m
	Wall thickness of pipe/outer pipe	t_p	0.00587	m
	Thermal conductivity of pipe/outer pipe wall	λ_p	2.0	$\mathrm{W\,m^{-1}\,K^{-1}}$
	Soil/rock thermal conductivity	λ_s	2.78	$\mathrm{W\,m^{-1}\,K^{-1}}$
	Heat capacity of soil/rock	$\rho_s c_s$	3.2×10^6	$\mathrm{J\,m^{-3}\,K^{-1}}$
	Thermal conductivity of grout	λ_g	1.7	$\mathrm{W\,m^{-1}\,K^{-1}}$
	Heat capacity of grout	$\rho_g c_g$	3.8×10^6	$\mathrm{J\,m^{-3}\,K^{-1}}$
	Thermal conductivity of circulation fluid	λ_f	0.59	$\mathrm{W\,m^{-1}\,K^{-1}}$
	Heat capacity of circulation fluid	$\rho_f c_f$	4.19×10^6	$\mathrm{J\,m^{-3}\,K^{-1}}$
	Dynamic viscosity of circulation fluid	μ_f	1.14×10^{-3}	$\mathrm{kg\,m^{-1}\,s^{-1}}$
	Flow rate of circulation fluid	Q_f	50	$\mathrm{m^3\,h^{-1}}$
DBHE only	Internal diameter of inner pipe	d_{pi}	0.09532	m
	Thermal conductivity of inner pipe wall	λ_{pi}	1.3	$\mathrm{W\,m^{-1}\,K^{-1}}$
	Wall thickness of inner pipe	t_{pi}	0.00734	m

Thermal Performance Test (TPT) [39]. This configuration is applied in scenarios 1A to 1D (see Table 3), and the simulated heat extraction rate is quantified based on the simulation results presented in section 4.1.

$$P_{\mathrm{EU}} = \rho_f c_f Q_f (T_o - T_i). \tag{8}$$

- Constant heat extraction rate

When an EUBHE system is in operation, it is very rare to have a fixed inflow temperature. Instead, the inflow temperature is dynamically adapted to the outflow temperature and the heat extraction rate imposed. When a fixed heat extraction rate is applied, it is ideally operated as a Thermal Response Test (TRT) [39]. To make the EUBHE run sustainably, the inflow temperature should always be kept above 0 °C, as water is commonly used as the circulation fluid. The circulation fluid temperature constraint can then be used to determine the maximum sustainable heat extraction rate P_{EU}^{m}. This type of boundary condition is applied in scenarios 2A to 2D (see Table 3) in order to quantify the maximum P_{EU}^{m} value. When the heat extraction rate is imposed in the simulation, the temperature difference between inflow and outflow is regulated according to Eq. (9),

$$T_i = T_o - \frac{P_{\mathrm{EU}}}{\rho_f c_f Q_f}. \tag{9}$$

- Constant building thermal power

  In a more realistic case, when EUBHE is constructed for building heating purposes, the heat pump is often installed to elevate the fluid temperature from the ground loop. Hence, the building thermal power is not equal to the heat extraction rate imposed on EUBHE. The performance of the heat pump can be quantified by the Coefficient of Performance (COP), which is defined as a ratio between the amount of thermal power supplied to the building P_{building} versus the amount of electric power consumed by the heat pump W_{hp}. With a constant building thermal power, the dynamic heat extraction rate on EUBHE, *i.e.* P_{EU} can be described as,

$$P_{\mathrm{EU}} = \frac{\mathrm{COP} - 1}{\mathrm{COP}} P_{\mathrm{building}}. \tag{10}$$

  Although a number of factors have an impact on the COP of a heat pump, it is widely accepted (*cf.* Casasso and Sethi [40] and Kahraman and Çelebi [41]) that a linear relationship can be established between the heat pump COP and the outflow temperature of EUBHE or DBHE (T_o).

$$\mathrm{COP} = aT_o + b. \tag{11}$$

  Here, a and b are constants under the specific operation model of heat pump. In this study, the COP curve is provided based on a designed floor heating temperature of 35 °C. The coefficients of Eq. (11) read $a = 0.083$, $b = 3.925$ for building heating (*cf.* Hein et al. [34], Zheng et al. [42]). Scenarios 5A and 5B (see Table 3) are configured with this type of boundary condition to evaluate the efficiency of the EUBHE system under the constant building thermal power.

3.2.3. Domain and meshing

When the EUBHE system is in operation, only the soil/rock in the vicinity of the boreholes will be affected. Therefore, all thermally undisturbed subsurface areas can be excluded from the finite element mesh of the EUBHE system. The mesh used in this work is constructed in two steps. In the first step, a 2D mesh is established with the borehole point. Following Diersch's approach [31, 30], the element size around the borehole is selected based on the radius of the borehole and the number of connecting nodes. According to the borehole radius listed in Table 2, the size of a typical triangular element in the vicinity of the borehole is chosen to be around 0.66 m. It is important to include sufficient subsurface areas in the model, so that the thermal plume will not interfere with the no-heat-flux boundaries. Therefore, several trial simulations with different lengths of operation time are performed to find out the influence range of the thermal plume. In these simulations, an annual heating season is set to 120 days followed by a 245-day long recovery period. The simulated soil/rock temperature distribution profile crossing the borehole at a depth of 1300 m is presented in Fig. 5. The thermally affected distance reaches around 30 m away from the borehole location after 4 years. After 10 years, the distance increases to around 70 m with specific properties listed in Table 2. The extent of the thermally affected zone along the borehole remains almost the same. Therefore, a cross-section of 100 $\times$ 100 m is chosen for the short-term (120 days) modelling domain in the vicinity of the borehole and 205 $\times$ 205 m for 10-year simulations to avoid the influence of the soil/rock boundary.

In the second step, the 2D mesh is further extruded along the trajectory of the two connected boreholes to form the 3D mesh. As for the vertical element size, a sensitivity analysis is also performed with a vertical length of 1, 5, 10, 20, and 50 m. All meshes are simulated for a single heating season (120 days). The outflow temperature difference is merely 0.011 °C at the end of the heating season. However, the computational time of the model with vertical elements size of 50 m is 8.47 % of that with the 10 m vertical resolution and 2.13 % of that with 1 m vertical resolution. In order to save computational time, the average vertical elements size is chosen to be 23.31 m (refined in the bottom) in the EUBHE model and 20 m in the DBHE model, leading to 116,183 prism and 223 line elements in the EUBHE model, and 97,090 prism elements and 130 line elements in the DBHE model accordingly.

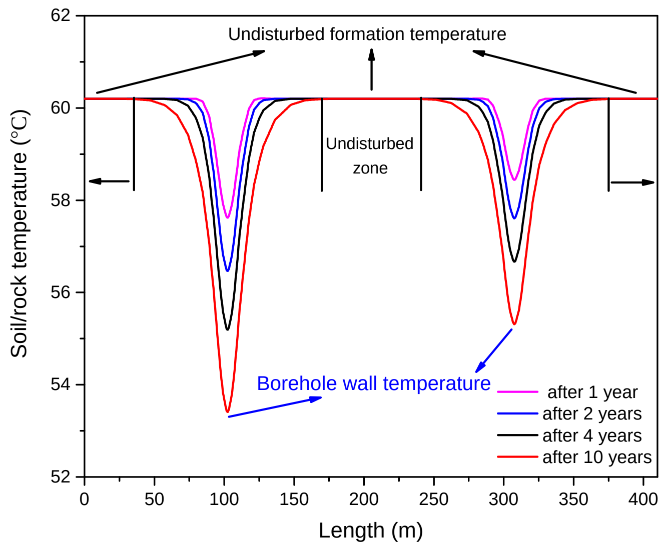

Figure 5: Extent of thermally affected zone at depth of 1300 m after operation of 1 year, 2 years, 4 years, and 10 years.

3.3. Simulation Scenarios

With the verified numerical model and domain mesh of the EUBHE system as described above, a series of scenarios are set up (see Table 3) and simulated. In the first step, our intention is to find out how much heat and at what extraction rate can an EUBHE system be sustainably operated over 120 days (a single heating season). To investigate this issue, scenarios 1A to 1D with four different constant inflow temperatures (5, 10, 15 and 20 °C) of the EUBHE system are set up to achieve different heat extraction rates. With these different inflow temperature, the range of heat extraction rate from the EUBHE system is calculated to be 0.82 MW to 1.13 MW (see section 4.1). Usually, the inflow temperature can never be constant. Hence, four scenarios 2A to 2D with different constant heat extraction rates, at 0.9, 1.0, 1.1 and 1.2 MW are set up. The evolution of both inflow and outflow temperatures is observed and presented in section 4.2 to evaluate the maximum sustainable heat extraction rate. Following this, the results from scenario 2B at a heat extraction rate of 1.0 MW are further analysed in section 4.3, where the spatial temperature distribution and heat flux distribution along the borehole are quantified. In scenarios 3A to 3D, the total borehole length of the EUBHE system is kept constant, while the ratios between the vertical and the horizontally deviated section are varied. The intention here is to figure out the optimal vertical/horizontal ratio leading to the best performance. The analysis is presented in section 4.4. Since the EUBHE system will be utilised for a very long period of time after construction, the circulation fluid temperature evolution in the long term is critical to its sustainability. Therefore, in the third step, scenarios 4A and 4B are simulated for an operation period of 10 years at the heat extraction rate of 1.0 MW and 1.1 MW, respectively. Meanwhile, the 2-DBHE array system is also operated for 10 years at 1.0 MW in scenario 4C, to compare its thermal performance with that of the EUBHE system. At last, their long-term efficiency for heating buildings is further analysed and compared in section 4.6.

Table 3: Overview of simulated scenarios and features.

Scenario ID	Inflow temperature (°C)	Heat extraction rate (MW)	Ratio of vertical to horizontal section	Operation time (day)
1A	5	-		
1B	10	-	12.2	120
1C	15	-		
1D	20	-		
2A	-	0.9		
2B	-	1.0	12.2	120
2C	-	1.1		
2D	-	1.2		
3A	-		46.9	
3B	-	1.0	12.2	120
3C	-		5.9	
3D	-		2.7	
4A	-	1.0	12.2	
4B	-	1.1	12.2	3650
4C / DBHE	-	1.0	-	
5A	-	Varies according to Eq. (10)	12.2	3650
5B / DBHE	-	Varies according to Eq. (10)	-	3650

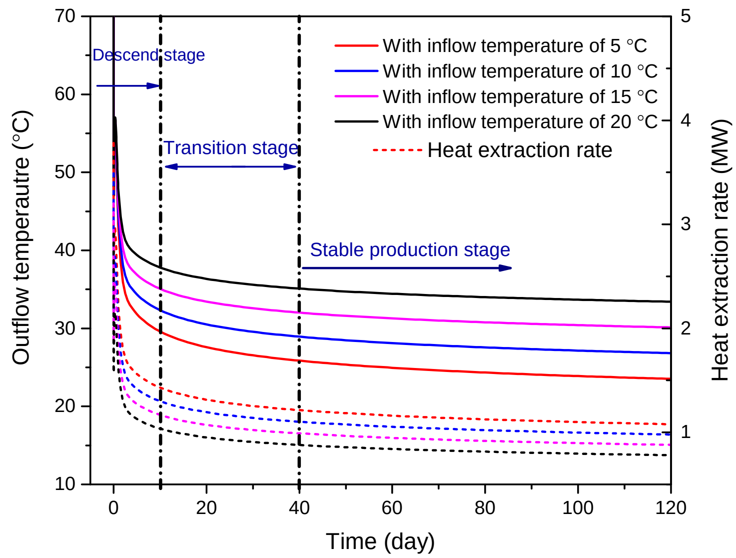

Figure 6: Changes of outflow temperature (solid line) and heat extraction rate (dash line) of the EUBHE system for four different inflow temperatures in a single heating season (120 days).

4. Results and discussions

4.1. Heat extraction rates of EUBHE with different inlet temperatures

As listed in Table 3, the Dirichlet-type boundary condition is imposed on the EUBHE system with constant inflow temperatures at 5, 10, 15 and 20 °C in scenarios 1A to 1D. These scenarios are simulated for a single heating season (120 days). The evolution of outflow temperature and heat extraction rate is presented in Fig. 6. Since the low-temperature fluid is injected continuously into the EUBHE, the outflow temperature drops rapidly in the beginning stage. After that, the outflow temperature decreases slowly (transition stage) and barely changes at the end of the heating season (stable production stage). When the inflow temperature increases from 5 °C up to 20 °C, the corresponding outflow temperature increases from 23.53 °C to 33.42 °C after the heating season. To the contrary, the temperature difference between outflow and inflow of the EUBHE decreases from 18.53, 16.83, 15.12 down to 13.42 °C at the end of the heating season. Since the heat extraction rate is calculated according to the inflow and outflow temperature, the calculated heat extraction rate decreases along with the elevated inflow temperature. In addition, the change of the heat extraction rate follows the same trend as that of the outflow temperature over time. From the 40-th day to the end of the heating season, the outflow temperature changes within a small range of 1.7 °C, which means the system has entered a stable production state (see Fig. 6). Therefore, the average stable heat extraction rate of the EUBHE system can be calculated over the entire stable production stage, which is calculated to be 1.13, 1.03, 0.92 and 0.82 MW under constant inflow temperatures at 5, 10, 15 and 20 °C.

4.2. Short-term performance under different heat extraction rates

In the previous thermal performance tests, the inflow temperature is imposed as the constant boundary condition. Hence, the calculated rate is limited by the inflow temperature. In order to investigate the maximum sustainable rate, thermal response tests as described in section 3.2.2 are conducted. In scenario 2A to 2D, the heat extraction rates are increased in four steps, from 0.9, 1.0, 1.1 up to 1.2 MW based on the TPT results. All these four scenarios are simulated one after the other for a single heating season (120 days). In a sustainable EUBHE system, the inflow and outflow temperatures should always be kept above 0 °C.

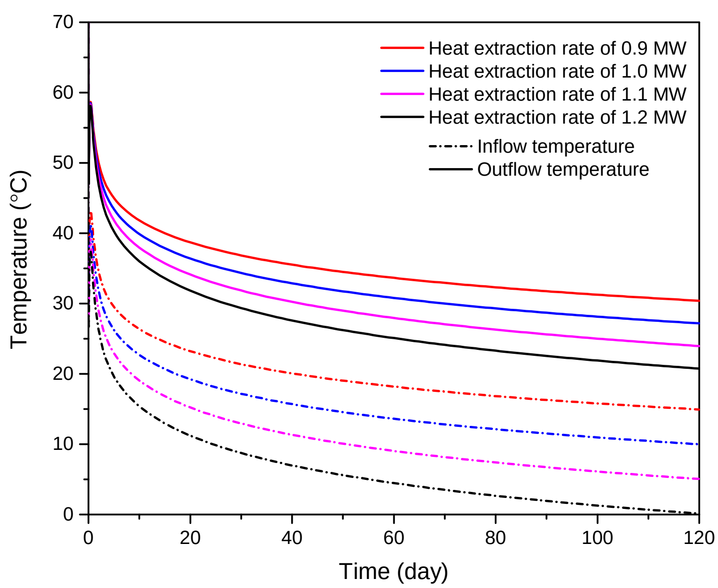

Figure 7: Inflow (dash-dot lines) and outflow (solid lines) temperatures of the EUBHE system for four different heat extraction rates in a single heating season.

The simulated inflow and outflow temperatures in a single heating season are presented in Fig. 7. With the increase in heat extraction rate, the inflow and outflow temperatures drop faster. For example, with 0.9 MW thermal load, the inflow temperature is 14.93 °C after the heating season. Increase of the heat extraction rate to 1.1 MW results in the inflow temperature drop down to 5.06 °C at the end of the heating season. If the heat extraction rate is further raised up to 1.2 MW, the same temperature approaches 0 °C after continuously operated for a single heating season. Further, under a heat extraction rate of 1.2 MW, the inflow temperature is 0.12 °C after 120 days. This operation mode may be impracticable in reality. However, the purpose here is to investigate the upper limit of the EUBHE system in terms of heat extraction rate through thermal response tests. That means the inflow temperature should be as low as possible, in this case just above the freezing point. This kind of thermal response test can help us to reveal the maximum sustainable heat extraction rate of the EUBHE system with water as the heat transport working fluid. It can be concluded, for the current EUBHE design in the short term, that 1.2 MW is the upper limit of the heat extraction rate.

4.3. Heat flux distribution along the boreholes

In a sustainable EUBHE system, *e.g.* scenario 2B, the specific heat extraction rate is 192.3 W/m. This value can be regarded as the averaged specific heat flux transferred from the grout to the circulation fluid. However, the averaged specific value does not reflect the flux distribution in the subsurface, let alone a varying re-distribution process over the entire heating season. In order to reveal this trend, the simulated temperature and heat flux distribution along the boreholes after operation of 1 day, 30 days and 120 days in scenario 2B are depicted in Fig. 8 for further analysis.

When the inflow temperature is higher than the soil/rock temperature, the heat stored in the circulation fluid is transferred to the surrounding soil/rock, resulting in the heat flux values being positive in the top of the downward inflow pipe at the beginning of the operation. The zero-heat-flux point in the downward inflow pipe is located at the depth of around 500 m after 1 day of operation (see Fig. 8(a)). At this depth, temperature of the circulation fluid reaches equilibrium with the surrounding soil/rock. Above it, heat will be dissipated into the subsurface. Below this point, as the temperature of the surrounding rock increases, the heat flux value becomes negative, indicating that the circulation fluid is being heated up.

However, the location of the zero-heat-flux point moves upwards as operational time progresses. It reaches the ground surface after operation of 30

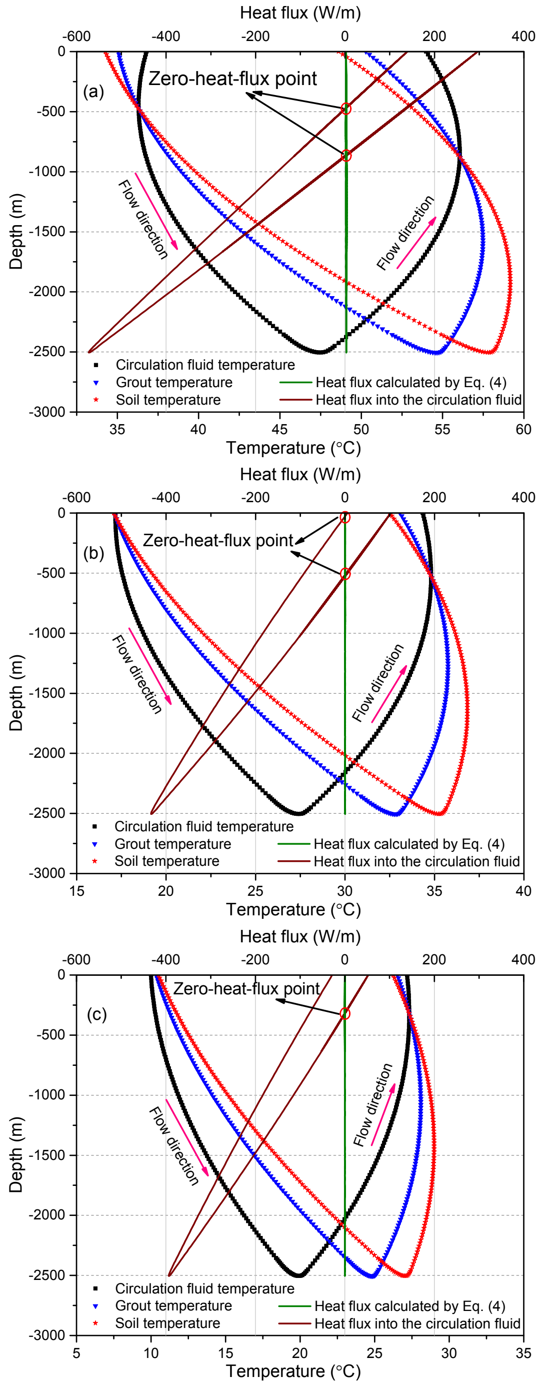

Figure 8: Distributions of temperatures and heat flux along the U-shaped borehole after operation of (a) 1 day, (b) 30 days, and (c) 120 days.

days as presented in Fig. 8(b). This is because the inflow temperature decreases over time when a continuous thermal load is imposed on the EUBHE as demonstrated in Fig. 7. Once the inflow temperature drops below the ground surface temperature (in Fig. 8(c)), the heat starts to be transferred from the soil/rock to the circulation fluid and the direction of heat flux is thus inverted, resulting in negative heat flux values at the top of the downward inflow pipe. This process shifts the zero-heat-flux point upwards. After *ca.* 40 days, this point disappears and the entire downward inflow pipe absorbs heat. To the contrary, in the upwards outflow pipe, as the circulation fluid is already heated up by the deep formation, the circulation fluid above the zero-heat-flux point is always hotter and dissipates heat to the shallow soil/rock. This suggests that the insulation layers should always be added to the upward outflow section of the EUBHE, in order to minimise the heat loss and improve the thermal performance.

When looking at the distribution of heat flux over depth, the temperature difference between soil/rock and circulation fluid is the greatest at the bottom section. At the depth of 2505 m, the ΔT value decreases from 10.35 °C to 7.12 °C after 120 days (see black and red scattered line in Fig. 8(a) and Fig. 8(c)). Although this decrease in ΔT causes the heat flux to decrease from 572.07 W/m after 1 day down to 392.96 W/m after 120 days, it is still much higher than the average value of 192.3 W/m, showing that the bottom section of the EUBHE has a much better thermal performance.

4.4. Ratio of deviated and vertical borehole sections

The above heat flux analysis raises an interesting question, *i.e.* whether it is possible to increase the system thermal performance of EUBHE by increasing the ratio of deep deviated section or the horizontal distance between two boreholes? In order to answer this question, four scenarios (3A to 3D) with different ratios of deviated and vertical sections are constructed while keeping the total borehole length unchanged. At the ground surface, the horizontal distance between two vertical boreholes is set to be 55, 205, 405 and 805 m, respectively. Following this design, the vertical depth of EUBHE system is set to be 2580, 2505, 2405 and 2205 m in scenario 3A to 3D accordingly (see Table 3). Other model parameters, such as the ground surface temperature and geothermal gradient are kept the same in these four scenarios, 1.0 MW heat extraction rate is equally imposed on each model, and all scenarios are simulated for the same heating season of 120 days.

The resulting inflow and outflow temperature profiles over time are depicted in Fig. 9. With the biggest horizontal distance between two boreholes at the surface, *i.e.* 805 m (scenario 3D), the outflow temperature at the end

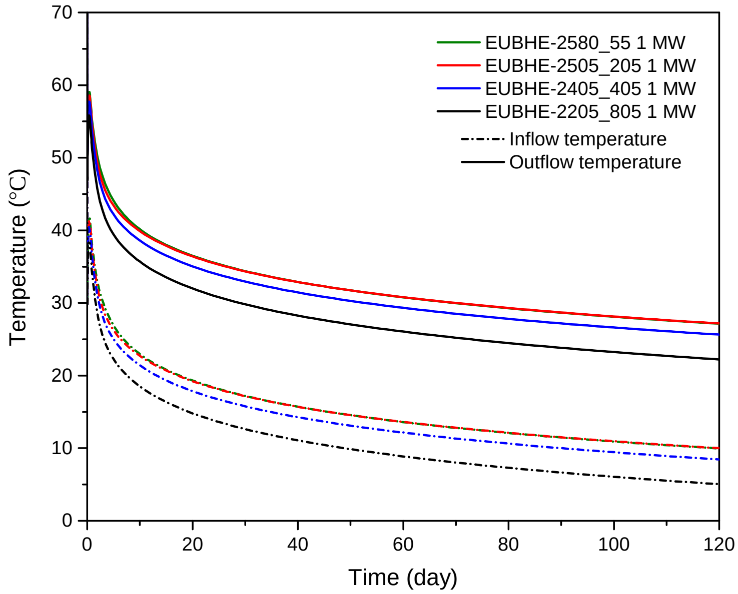

Figure 9: Inflow (dash-dot lines) and outflow (solid lines) temperatures for four EUBHE systems with different ratios of vertical depth and horizontal distance.

of the heating season is 22.23 °C. When the horizontal distance decreases to 405 m with a vertical depth of 2405 m (scenario 3C), the outflow temperature increases to 25.64 °C at the end of 120 days. However, when the horizontal section is further deceased from 205 m in scenario 3B to 55 m in scenario 3A, the outflow temperature decreases by 0.04 °C and approaches 27.14 °C at the end of the heating season in scenario 3A. It can be found that increasing depth of vertical section can lead to a better thermal performance rather than extending the length of the horizontal section. This is because the temperature difference between circulation fluid and soil/rock is higher in the deeper formation, so that more heat transfer can be achieved there. With the constraint on total borehole length, a 205 m surface distance between the two boreholes produces the best heat extraction rate. With a shorter distance, *e.g.* 55 m, the short-term heat extraction rate decreases slightly. Nevertheless, the long-term heat extraction rate may decline considerably over a span of 10 to 15 years due to the thermal interactions between two boreholes.

4.5. Long-term thermal performance of EUBHE and 2-DBHE array

When an EUBHE system is constructed, it is planned to operate for more than 10 years. After the EUBHE system has operated for 120 days every year, the soil/rock temperature around the borehole can hardly be fully recovered in the following 245 days until the beginning of the next heating season. Thus, long-term operation of the EUBHE system needs to be continuously simulated to investigate its sustainability. In the long-term simulations over 10 years, the geometry of the soil/rock domain has been increased to include a cross section of 205×205 m surrounding the EUBHE to ensure that there is no interference caused by the boundary effect. In every heating season (120 days), the constant heat extraction rates at 1.0 MW and 1.1 MW are imposed in scenarios 4A and 4B, respectively. The heating season is followed by a recovery period of 245 days every year. Meanwhile, in order to compare the long-term performance with the 2-DBHE array system, a separate model with two DBHEs connected in parallel is also simulated for the same period of time. Thus, on each of the DBHEs, the heat extraction rate of 0.5 MW is imposed over the same heating season.

Figure 10 depicts the outflow and inflow temperatures of the EUBHE system in 10 years. It is found that temperatures of inflow and outflow at the end of each heating season decrease gradually. However, the decrements become smaller as the operational time progresses. For example, in scenario 4A, the outflow temperature at the end of the second heating season decreases by 1.52 °C compared with that of the first heating season, while it drops only 0.19 °C from the end of the 9th to the 10th heating season. Additionally, with a higher heat extraction rate imposed on the EUBHE system, the temperature difference between inflow and outflow over the entire heating season becomes greater under the same flow rate of the circulation fluid. The temperature difference is 17.18 °C under the heat extraction rate of 1.0 MW, while it becomes 18.90 °C under 1.1 MW, causing the temperatures to fall fast. Overall, both 1.0 MW and 1.1 MW heat extraction rates can be considered sustainable. In the 1.0 MW case (scenario 4A), the inflow and outflow temperature at the end of the 10th heating season are 5.94 °C and 23.13 °C, respectively. With a heat extraction rate of 1.1 MW (scenario 4B), the inflow temperature value is at 0.60 °C, indicating that the EUBHE system is operating close to its upper limit.

As for the 2-DBHE array, the simulated inflow and outflow temperatures are presented in Fig. 11. The temperature evolution follows a similar trend as in the EUBHE system. The outflow temperature difference between the end of 9th and 10th heating season is only 0.19 °C, suggesting that the heat

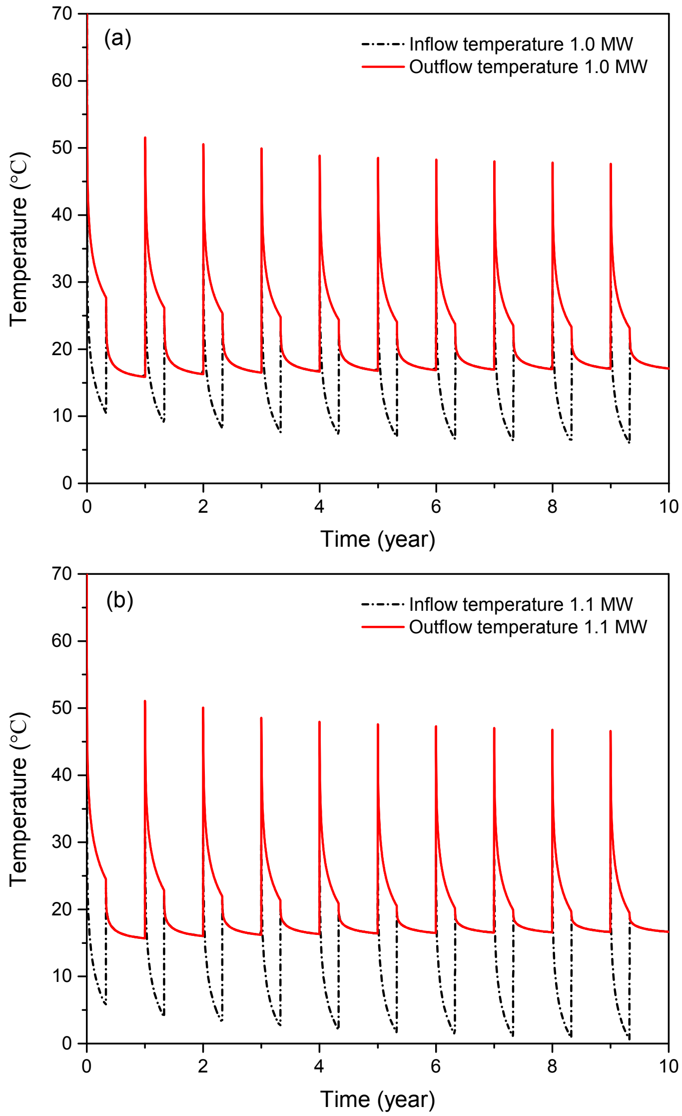

Figure 10: Inflow (dash-dot lines) and outflow (solid lines) temperatures of the EUBHE system over operation of 10 years at heat extraction rates of (a) 1.0 MW and (b) 1.1 MW.

transfer has reached a quasi-steady state. Meanwhile, the inflow temperature at the end of 10th season remains at 3.45 °C. These results suggest that the 2-DBHE can also be sustainably operated with a heat extraction rate of 1.0 MW over 10 years. In comparison, the EUBHE system clearly has a better performance: with a heat extraction rate of 1.0 MW, its outflow temperature is 11.09 °C higher than the 2-DBHE array system after operation of 10 years. From the economical point of view, this higher outflow temperature will lead to more savings in electricity consumed by the heat pump. Additionally, it can be seen from Fig. 11 that the heat extraction rate of 1.0 MW almost reaches the upper limit of the 2-DBHE array system. Overall, the EUBHE system can support a larger sustainable heat extraction rate than the 2-DBHE array system.

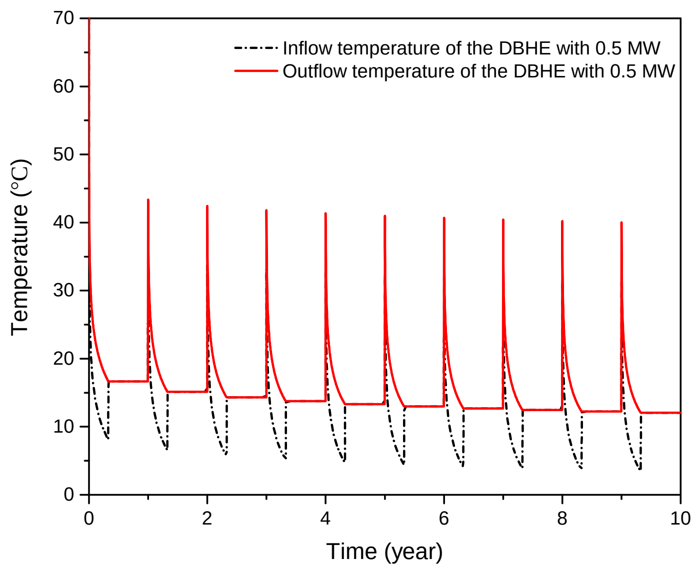

Figure 11: Inflow (dash-dot lines) and outflow (solid lines) temperatures of the single DBHE system over operation of 10 years at the heat extraction rate of 0.5 MW.

4.6. Efficiency comparison between EUBHE and 2-DBHE array systems

The operational costs of both the EUBHE system and the DBHE arrays system are largely composed of two types of electricity consumption: one from the heat pump and the other from the circulation pump. Following our previous work [6], the system efficiencies of the EUBHE and 2-DBHE array are quantified and compared using the Coefficient of System Performance (CSP), which is defined as,

$$\mathrm{CSP} = \frac{P_{\text{building}}}{\dot{W}_{hp} + \dot{W}_{cp}}. \tag{12}$$

The electric power of the heat pump $\dot{W}_{hp}$ can be further computed by its COP values and the transient heat extraction rate imposed on BHE (following Hein et al. [34] and Zheng et al. [42]),

$$\dot{W}_{hp}(t) = \frac{P_{\mathrm{BHE}}(t)}{COP(t)}. \tag{13}$$

where $P_{\mathrm{BHE}}(t)$ is the transient heat extraction rate imposed on DBHE or EUBHE. The electric power consumed by the circulation pump is a combination of borehole structure with the circulation fluid flow rate Q_f [13],

$$\dot{W}_{cp} = \frac{Q_f}{\eta}\left(\frac{L}{D_h}\frac{\rho_f Q_f^2}{2A^2}\frac{1}{(0.790\ln(\mathrm{Re}) - 1.64)^2}\right). \tag{14}$$

Here η is the efficiency of the circulation pump, assumed to be 70 %. Re is the Reynolds number. L denotes the borehole length, D_h is the hydraulic diameter of pipe and A is the pipe cross-section area. With the above relationship available, the total amount of electricity consumption (W) over operational time can be calculated by integrating the dynamic electric power,

$$W = \int_0^{t_{\mathrm{end}}} \left[\dot{W}_{hp}(t) + \dot{W}_{cp}\right] \,\mathrm{d}t. \tag{15}$$

In order to compare the long-term system efficiency for building heating either by EUBHE or 2-DBHE array, scenarios 5A and 5B are set up. Here both systems are employed to supply heating to a floor area of 35 000 m^2 for residential buildings in northern China. With an averaged outdoor air temperature of −9 °C and the indoor air temperature kept at 18 °C. According to the code for urban heating supply planning (GB/T 51074) [43], the specific thermal power value of the residential buildings in Beijing ranges from 30 to 36 $\mathrm{W/m}^2$ over the entire heating season. Here with a value of 35 $\mathrm{W/m}^2$, the total required thermal power is accounted to be 1.225 MW from the building side. By including the heat pump into the numerical model (see section 3.2.2), both EUBHE and 2-DBHE array systems are simulated for a 10-year period. In the DBHE array system, the two boreholes are parallelly connected. Thus, the total building thermal power is evenly divided, with 0.6125 MW on each DBHE.

The CSP values in each heating season are compared and presented in Fig. 12(a) with box plots, and the total electricity consumption is presented in Fig. 12(b). It can be found from Fig. 12(a) that the CSP values of the EUBHE system are consistently higher than that of the DBHE array in each of the 10 heating seasons. The average CSP value of the EUBHE system in

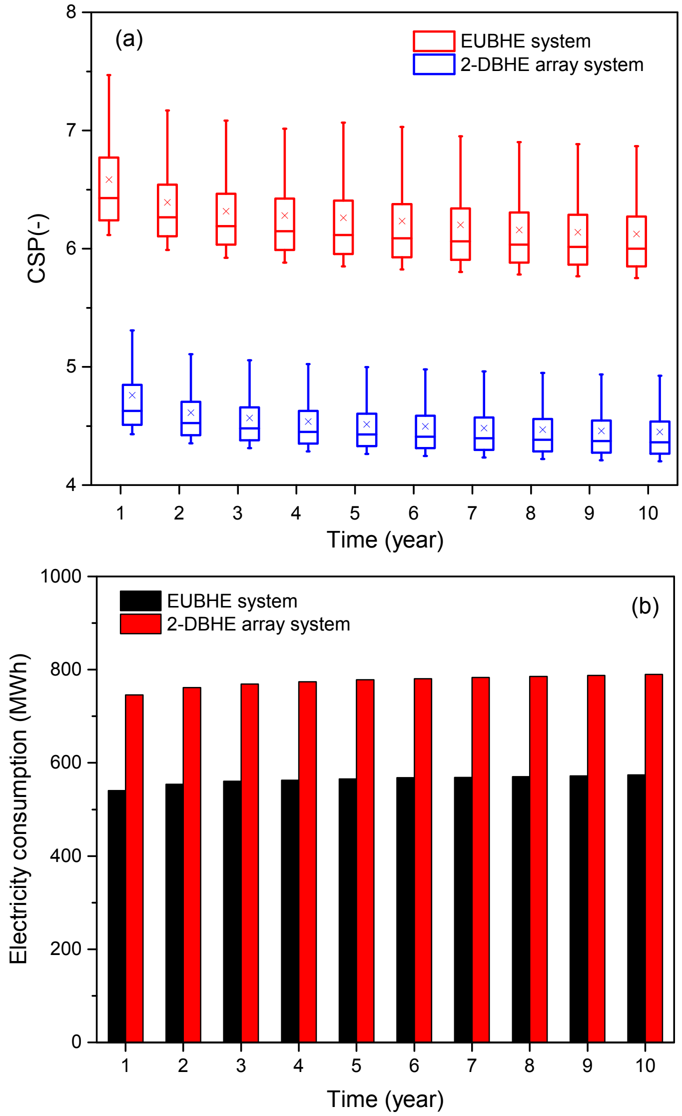

Figure 12: Efficiency comparison between the EUBHE system and the 2-DBHE array system when coupled with GSHP for building heating over the operation of 10 years. (a) The box plot of the CSP values, and (b) power consumption at every heating season.

the first heating season is 6.59, while it is only 4.76 in the DBHE array. The difference of average CSP value between two systems stays at 1.66 after 10 heating seasons. Such difference is mainly caused by the outflow temperature difference. To be specific, the outflow temperature of the EUBHE system at the end of the first heating season is 27.03 °C, which is 10.24 °C higher than that from the DBHE array. This trend is consistent over 10 years.

The electricity consumption presented in Fig. 12(b) shows that the EUBHE system is always more efficient than the 2-DBHE array. The EUBHE system uses 540.56 MWh electricity in the first heating season, which is 205.29 MWh less than the 2-DBHE array. As operational time increases, the EUBHE consumption gradually increases to 574.15 MWh in the 10th heating season, that is still 215.91 MWh (or about 27 %) less than the DBHEs. When looking into the origin of electricity consumption, the circulation pump in the EUBHE system needs 4.83 MWh in every heating season, while it is considerably higher (up to 132.77 MWh) in the 2-DBHE array system. The heat pump, in the first year for example, consumes 535.72 MWh (99.1 % of the total consumed electricity in the first heating season) in the EUBHE system and 613.08 MWh (82.2 % of the total consumed electricity in the first heating season) in the 2-DBHE array. Overall, the EUBHE system has higher efficiency with lower energy consumed by the heat pump and circulation pump, compared with the 2-DBHE array system.

4.7. Comparison and discussion on existing work of similar EUBHE systems

In applications of closed loop systems to extract deep geothermal energy, most of engineers and researchers focused on DBHE systems. Some representative applications and literature of reporting the capacity of DBHE systems are selected and compared in Table 4. It can be found that the DBHE specific heat extraction rate can hardly reach 200 W/m, while for the EUBHE system in this work, the sustainable heat extraction rate is found to be 211.5 W/m without further optimisation. For densely populated neighbourhoods, the heating demand cannot be satisfied by a single DBHE coupled GSHP system. Therefore, some engineers choose to increase the numbers of DBHE following the same idea as designing shallow BHE arrays [35]. However, DBHE has unavoidable structural limitation of extracting deep geothermal energy due to its coaxial pipe as stated in the Introduction section. Some researchers started to explore other high-efficiency closed loop systems for deep geothermal exploitation, for example, Song et al. [21] analysed the heat production performance of a closed loop geothermal system that has a horizontal borehole with a length of more than 7 km to connect two 3.5 km deep vertical boreholes. They concluded that the thermal power can reach more than 2 MW over 20 years. However, due to very high drilling cost of the horizontal boreholes, such large closed loop systems are not likely to be constructed in reality for heating neighbourhoods. Despite Li et al. [44, 9, 23] having reported the EUBHE system and studied the heat transfer characteristics, the efficiency analysis when using EUBHE coupled with GSHP systems for heating neighbourhoods is still lacking. From a construction perspective, EUBHE includes a deviated deep borehole and a connection with another vertical deep borehole at the bottom. This will undoubtedly increase the initial investment compared with 2-DBHE array systems. Therefore, it is very much needed to evaluate which benefits can be obtained by using EUBHE systems for building heating. From the analysis in Sections 4.5 and 4.6, the EUBHE system has better thermal performance and capacity than the 2-DBHE array system. Even providing heating for the same building areas, the total electricity consumption of the EUBHE coupled with GSHP system decreases by around 27 %. If the savings are higher than the additional initial investment, then the EUBHE system should be the preferred construction for heating densely populated neighbourhoods.

Table 4: Simple review on capacity of closed loop systems for deep geothermal energy exploitation.

Application / Reference	Depth (m)	Bottom temperature (°C)	Specific heat extraction rate (W/m)
Penzlau [45]	2786	108	53.8
Aachen [46]	2500	85	46.8
Weissbad [47]	1200	45	66.7
Weggis [48]	2300	78	43.5
Hawaii [49]	1962	110	188.8
Kong et al. [27]	2000	75	150
Chen et al. [6]	2600	84	125
Le Lous et al. [14]	5000	160	120
Wang et al. [8]	2000	75.6	143.2
Dai et al. [50]	1780	64	151.69
Fang et al. [51]	2000	70	100
This study	2505	102.375	211.5

5. Conclusions and outlook

In this work, a deep EUBHE system has been introduced to extract deep geothermal energy for building heating in densely populated neighbourhoods. In order to evaluate the system thermal capacity and efficiency compared with 2-DBHE array systems, a 3D EUBHE numerical model has been established using OGS software based on the geological conditions in northern China. The maximum sustainable heat extraction rate of the EUBHE system has been evaluated in short and long terms. The 10-year system thermal performance and efficiency have also been compared with the 2-DBHE array system when coupled with GSHP for building heating. The key findings of this study are as follows:

- The thermal performance tests and thermal response tests indicate that the maximum heat extraction rate of the EUBHE system is 1.2 MW in a single heating season. Considering thermal performance decline in long-term operation, the upper limit of sustainable heat extraction rate is 1.1 MW in 10 years. The system thermal performance can be improved by adding an insulation layer on the top of the outflow pipe.

- Under the same total borehole length, the EUBHE system performance can be improved by increasing the depth of vertical section instead of extending horizontal section. However, it is noted that, in the current design, the horizontal section should not be less than 55 m to prevent thermal interaction between neighbouring boreholes.

- The EUBHE system is more efficient than the 2-DBHE array system when coupled with GSHP for building heating under the same total borehole length. For the thermal power of 1.225 MW from the building site, the total electricity consumed by the present EUBHE system is approximately 27 % less than that by the 2-DBHE array system in 10 years. And the average CSP value of the EUBHE system is 1.66 higher over 10 heating seasons.

Although the EUBHE system has been predicted to have better thermal performance and higher efficiency than the 2-DBHE array system, it might need higher initial investment in constructing the deviated borehole and the corresponding connection. For the economical feasibility of the EUBHE system application in real building heating projects, it is important to obtain more cost information and compare it with the savings from the long-term operation. In addition, the EUBHE system performance can be influenced by soil/rock properties, borehole structures, pipe and grout properties, and flow rate of the circulation fluid. The specific influence of these parameters will be discussed in a system optimisation study in the future.

CRediT authorship contribution statement

Chaofan Chen: Conceptualization, Methodology, Software, Validation, Writing - Original Draft. **Wanlong Cai:** Formal analysis, Visualization. **Dmitri Naumov:** Software, Data Curation. **Kun Tu:** Formal analysis. **Hongwei Zhou:** Resources, Supervision. **Yuping Zhang:** Investigation, Conceptualization. **Olaf Kolditz:** Project administration, Supervision. **Haibing Shao:** Methodology, Software, Writing - Review & Editing, Supervision.

Declaration of competing interest

The authors declare that they have no known competing financial interests or personal relationships that could have appeared to influence the work reported in this paper.

Acknowledgements

The research work is part of the new Helmholtz Research Program "Changing Earth – Sustaining our Future" Topic 8 "Geo-resources for the Energy Transition and a High-Tech Society" within the program-oriented research (POF IV). This work is also part of the EASyQuart project "Energy-efficient design and planning of decentralised supply networks for heating and cooling of urban areas using the shallow subsurface" funded by the Federal Ministry for Economic Affairs and Energy (Grant No 03EGB0016C) which is gratefully acknowledged. This work also receives partial funding from the Sha'anxi Province Natural Science Foundation Project (No. 2020JM-717) and Xi'an Social Development Science and Technology Innovation Demonstration Project (No. 20SFSF0017). In addition, the first author (Chaofan Chen) would like to acknowledge the China Scholarship Council (CSC) for financially supporting his PhD study in Germany. Special thanks to Ms. Leslie Jakobs for thoroughly proofreading the manuscript.

References

[1] S. S. Naicker, S. J. Rees, Long-term high frequency monitoring of a large borehole heat exchanger array, Renewable Energy 145 (2020) 1528–1542.

[2] C. Zhang, Y. Wang, Y. Liu, X. Kong, Q. Wang, Computational methods for ground thermal response of multiple borehole heat exchangers: A review, Renewable Energy 127 (2018) 461–473.

[3] S. Chen, W. Cai, F. Witte, X. Wang, F. Wang, O. Kolditz, H. Shao, Long-term thermal imbalance in large borehole heat exchangers array-a numerical study based on the leicester project, Energy and Buildings (2020) 110518.

[4] W. Cai, F. Wang, J. Liu, Z. Wang, Z. Ma, Experimental and numerical investigation of heat transfer performance and sustainability of deep borehole heat exchangers coupled with ground source heat pump systems, Applied Thermal Engineering 149 (2019) 975–986.

[5] J. Liu, F. Wang, W. Cai, Z. Wang, C. Li, Numerical investigation on the effects of geological parameters and layered subsurface on the thermal performance of medium-deep borehole heat exchanger, Renewable Energy 149 (2020) 384–399.

[6] C. Chen, H. Shao, D. Naumov, Y. Kong, K. Tu, O. Kolditz, Numerical investigation on the performance, sustainability, and efficiency of the deep borehole heat exchanger system for building heating, Geothermal Energy 7 (2019) 18.

[7] S. Pan, Y. Kong, C. Chen, Z. Pang, J. Wang, Optimization of the utilization of deep borehole heat exchangers, Geothermal Energy 8 (2020) 6.

[8] Z. Wang, F. Wang, J. Liu, Z. Ma, E. Han, M. Song, Field test and numerical investigation on the heat transfer characteristics and optimal design of the heat exchangers of a deep borehole ground source heat pump system, Energy Conversion and Management 153 (2017) 603–615.

[9] C. Li, Y. Guan, X. Wang, C. Zhou, Y. Xun, L. Gui, Experimental and numerical studies on heat transfer characteristics of vertical deep-buried u-bend pipe in intermittent heating mode, Geothermics 79 (2019) 14–25.

[10] S.-U. Schulz, Investigations on the improvement of the energy output of a Closed Loop Geothermal System (CLGS), Ph.D. thesis, Technische Universität Berlin, 2008.

[11] C. Li, Y. Guan, C. Jiang, S. Deng, Z. Lu, Numerical study on the heat transfer, extraction, and storage in a deep-buried pipe, Renewable Energy 152 (2020) 1055–1066.

[12] Eavor Technologies Inc., `https://eavor.com/`, 2020. Accessed: 2020-06-29.

[13] H. Holmberg, J. Acuña, E. Næss, O. K. Sønju, Thermal evaluation of coaxial deep borehole heat exchangers, Renewable Energy 97 (2016) 65–76.

[14] M. Le Lous, F. Larroque, A. Dupuy, A. Moignard, Thermal performance of a deep borehole heat exchanger: Insights from a synthetic coupled heat and flow model, Geothermics 57 (2015) 157–172.

[15] H. Ramey Jr, et al., Wellbore heat transmission, Journal of petroleum Technology 14 (1962) 427–435.

[16] A. Hasan, C. Kabir, M. Ameen, et al., A fluid circulating temperature model for workover operations, SPE Journal 1 (1996) 133–144.

[17] P. Eskilson, Thermal analysis of heat extraction boreholes, Ph.D. thesis, University of Lund, 1987.

[18] B. Dehghan, E. Kukrer, A new 1d analytical model for investigating the long term heat transfer rate of a borehole ground heat exchanger by green's function method, Renewable Energy 108 (2017) 615–621.

[19] R. A. Beier, Transient heat transfer in a u-tube borehole heat exchanger, Applied thermal engineering 62 (2014) 256–266.

[20] R. A. Beier, J. Acuña, P. Mogensen, B. Palm, Transient heat transfer in a coaxial borehole heat exchanger, Geothermics 51 (2014) 470–482.

[21] X. Song, Y. Shi, G. Li, Z. Shen, X. Hu, Z. Lyu, R. Zheng, G. Wang, Numerical analysis of the heat production performance of a closed loop geothermal system, Renewable Energy 120 (2018) 365–378.

[22] G. Cui, S. Ren, L. Zhang, J. Ezekiel, C. Enechukwu, Y. Wang, R. Zhang, Geothermal exploitation from hot dry rocks via recycling

heat transmission fluid in a horizontal well, Energy 128 (2017) 366–377.

[23] C. Li, Y. Guan, X. Wang, Study on reasonable selection of insulation depth of the outlet section of vertical deep-buried u-bend tube heat exchanger, Energy and Buildings 167 (2018) 231–239.

[24] F. Tang, H. Nowamooz, Long-term performance of a shallow borehole heat exchanger installed in a geothermal field of alsace region, Renewable Energy 128 (2018) 210–222.

[25] B. Larwa, K. Kupiec, Heat transfer in the ground with a horizontal heat exchanger installed–long-term thermal effects, Applied Thermal Engineering 164 (2020) 114539.

[26] T. Renaud, P. Verdin, G. Falcone, Numerical simulation of a deep borehole heat exchanger in the krafla geothermal system, International Journal of Heat and Mass Transfer 143 (2019) 118496.

[27] Y. Kong, C. Chen, H. Shao, Z. Pang, L. Xiong, J. Wang, Principle and capacity quantification of deep-borehole heat exchangers, Chinese Journal of Geophysics-Chinese Edition 60 (2017) 4741–4752.

[28] R. Al-Khoury, T. Kölbel, R. Schramedei, Efficient numerical modeling of borehole heat exchangers, Computers & Geosciences 36 (2010) 1301–1315.

[29] H.-J. Diersch, D. Bauer, W. Heidemann, W. Rühaak, P. Schätzl, Finite element modeling of borehole heat exchanger systems: Part 1. fundamentals, Computers & Geosciences 37 (2011) 1122–1135.

[30] H. Diersch, D. Bauer, W. Heidemann, W. Rühaak, P. Schätzl, et al., Finite element modeling of borehole heat exchanger systems: Part 2. numerical simulation., Computers & Geosciences 37 (2011) 1136–1147.

[31] H.-J. G. Diersch, FEFLOW: finite element modeling of flow, mass and heat transport in porous and fractured media, Springer Science & Business Media, 2013.

[32] O. Kolditz, S. Bauer, L. Bilke, N. Böttcher, J.-O. Delfs, T. Fischer, U. J. Görke, T. Kalbacher, G. Kosakowski, C. McDermott, et al., OpenGeoSys: an open-source initiative for numerical simulation of thermo-hydro-mechanical/chemical (THM/C) processes in porous media, Environmental Earth Sciences 67 (2012) 589–599.

[33] H. Shao, P. Hein, A. Sachse, O. Kolditz, Geoenergy Modeling II: Shallow Geothermal Systems, Springer, 2016.

[34] P. Hein, O. Kolditz, U.-J. Görke, A. Bucher, H. Shao, A numerical study on the sustainability and efficiency of borehole heat exchanger coupled ground source heat pump systems, Applied Thermal Engineering 100 (2016) 421–433.

[35] S. Chen, F. Witte, O. Kolditz, H. Shao, Shifted thermal extraction rates in large borehole heat exchanger array–a numerical experiment, Applied Thermal Engineering 167 (2020) 114750.

[36] Y. Huang, Y. Zhang, Y. Xie, Y. Zhang, X. Gao, Thermal performance analysis on the composition attributes of deep coaxial borehole heat exchanger for building heating, Energy and Buildings 221 (2020) 110019.

[37] C. Chen, H. Shao, Wellbore Heat Transport - EUBHE, `https://www.opengeosys.org/docs/benchmarks/heat-transport-bhe/pipe_flow_ebhe/`, 2020. Accessed: 2020-06-29.

[38] Y. Zhang, S. Huang, F. Yang, X. Wang, R. Yu, Y. Li, Y. Xun, C. Zhou, Geothermal features of two deep U-shape Downhole Heat Exchangers in the Xi'an depression, Guanzhong Basin, Coal Geology of China 31 (2019) 54–61.

[39] W. Choi, H. Kikumoto, R. Ooka, Critical comparison between thermal performance test (TPT) and thermal response test (TRT): Differences in heat transfer process and extractable information, Energy Conversion and Management 199 (2019) 111967.

[40] A. Casasso, R. Sethi, Efficiency of closed loop geothermal heat pumps: A sensitivity analysis, Renewable Energy 62 (2014) 737–746.

[41] A. Kahraman, A. Çelebi, Investigation of the performance of a heat pump using waste water as a heat source, Energies 2 (2009) 697–713.

[42] T. Zheng, H. Shao, S. Schelenz, P. Hein, T. Vienken, Z. Pang, O. Kolditz, T. Nagel, Efficiency and economic analysis of utilizing latent heat from groundwater freezing in the context of borehole heat exchanger coupled ground source heat pump systems, Applied Thermal Engineering 105 (2016) 314–326.

[43] GB/T 51074, Code for urban heating supply planning, Ministry of Housing and Urban-Rural Development, PR China, 2015.

[44] C. Li, Y. Guan, X. Wang, G. Li, C. Zhou, Y. Xun, Experimental and numerical studies on heat transfer characteristics of vertical deep-buried u-bend pipe to supply heat in buildings with geothermal energy, Energy 142 (2018) 689–701.

[45] A. Sapinska-Sliwa, M. A. Rosen, A. Gonet, T. Sliwa, Deep borehole heat exchangers—a conceptual and comparative review, International Journal of Air-Conditioning and Refrigeration 24 (2016) 1630001.

[46] L. Dijkshoorn, S. Speer, R. Pechnig, Measurements and design calculations for a deep coaxial borehole heat exchanger in aachen, germany, International Journal of Geophysics 2013 (2013).

[47] T. Kohl, M. Salton, L. Rybach, Data analysis of the deep borehole heat exchanger plant weissbad (switzerland), in: Proceedings world geothermal congress, pp. 3459–3464.

[48] T. Kohl, R. Brenni, W. Eugster, System performance of a deep borehole heat exchanger, Geothermics 31 (2002) 687–708.

[49] K. Morita, W. S. Bollmeier, H. Mizogami, An experiment to prove the concept of the downhole coaxial heat exchanger (dche) in hawaii (1992).

[50] C. Dai, Y. Shi, L. Zeng, J. Li, H. Lei, Heat extraction performance of a deep downhole heat exchanger, Energy Procedia 158 (2019) 5602–5607.

[51] L. Fang, N. Diao, Z. Shao, K. Zhu, Z. Fang, A computationally efficient numerical model for heat transfer simulation of deep borehole heat exchangers, Energy and Buildings 167 (2018) 79–88.

[52] V. Gnielinski, New equations for heat and mass transfer in the turbulent flow in pipes and channels, NASA STI/recon technical report A 75 (1975) 8–16.

[53] S. W. Churchill, Comprehensive correlating equations for heat, mass and momentum transfer in fully developed flow in smooth tubes, Industrial & Engineering Chemistry Fundamentals 16 (1977) 109–116.

Appendix A. Ramey's analytical solution

In Ramey's analytical solution, the outflow temperature of the pipe $T_o(t)$ inside the borehole can be expressed as a function of depth Δz and time t,

$$T_o(t) = T_s + (T_i(t) - T_s)\exp(-\Delta z/X) \tag{A.1}$$

where, $T_i(t)$ is the inflow temperature, T_s is the soil/rock temperature, and coefficient X is determined by,

$$X = \frac{Q\rho_f c_f(\lambda_s + r_p U f(t))}{2\pi r_p U \lambda_s} \tag{A.2}$$

here Q is the flow rate of the fluid in the pipe.

With dimensionless time $t_D = {}^{\lambda_s t}/_{(\rho_s c_s r_b^2)}$, the time function $f(t)$ is given as,

$$f(t) = [0.4063 + 0.5\ln(t_D)][1 + \frac{0.6}{t_D}] \qquad t_D > 1.5, \tag{A.3}$$

$$f(t) = 1.1281\sqrt{t_D}(1 - 0.3\sqrt{t_D}) \qquad t_D \leqslant 1.5, \tag{A.4}$$

and the overall heat transfer coefficient U is,

$$U = \left[\frac{r_p + t_p}{r_p h} + (r_p + t_p)(\frac{\ln\frac{r_p+t_p}{r_p}}{\lambda_p} + \frac{\ln\frac{r_b}{r_p+t_p}}{\lambda_g})\right]^{-1} \tag{A.5}$$

$$h = \frac{\lambda_f \mathrm{Nu}}{2r_p} \tag{A.6}$$

where, t_p is pipe wall thickness and r_p is internal radius of the pipe and r_b is radius of the borehole.

The Nusselt number can be determined according to the Gnielinski's equation [52],

$$\mathrm{Nu} = 4.364 \qquad \mathrm{Re} < 2300, \tag{A.7}$$

$$\mathrm{Nu} = \frac{{}^{f}/_{8}(\mathrm{Re} - 1000)\mathrm{Pr}}{1 + 12.7\sqrt{{}^{f}/_{8}}(\mathrm{Pr}^{2/3} - 1)} \qquad 2300 \leqslant \mathrm{Re} < 5 \times 10^6, \tag{A.8}$$

Pr is the Prandtl number, and the friction factor f is evaluated by Churchill correlation [53],

$$f^{-1} = \left(\frac{1}{\left[\left(\left(\frac{8}{\mathrm{Re}}\right)^{10} + \left(\frac{\mathrm{Re}}{36500}\right)^{20} \right) \right]^{1/2}} + \left[2.21 \left(\ln \frac{\mathrm{Re}}{7} \right) \right]^{10} \right)^{1/5} \tag{A.9}$$

The Prandtl and Reynolds number are defined as,

$$\mathrm{Pr} = \frac{\mu_f c_f}{\lambda_f} \qquad \mathrm{Re} = \frac{\rho_f v_f d_p}{\mu_f} \tag{A.10}$$

where, μ_f is the circulation fluid dynamic viscosity, ρ_f is the circulation fluid density, λ_f is the circulation fluid thermal conductivity, and c_f is the specific heat capacity of circulation fluid.